Spin and Angle Resolved Photoemission Setup: First Results

K. Hricovini[1,2], C. Richter[1,6], O. Heckmann[1],
P. Thiry[3], G. Jezequel[4], Y. Petroff[5],
G. Lampel[6], M. Campbell[7]

[1]LMPS, Université de Cergy-Pontoise, Neuville/Oise, 95031 Cergy-Pontoise
[2]LURE, Bat. 209 d, 91 898 Orsay
[3]ESRF, Grenoble
[4]Université de Rennes1
[5]Ministère de la Recherche, Paris
[6]PMC, Ecole Polytechnique, Palaiseau
[7]University of Edinburgh, Great Britain

1. Introduction

Here we present first results obtained on the spin and angle-resolved phtotoemission setup first developed in LURE (Y.Petroff, P. Thiry, G. Jezequel) and then in LPMS (Université de Cergy-Pontoise) in collaboration with University of Edinburgh and PMC (Ecole Polytechnique) laboratories. The measurements have been performed in summer 2003 on the SU6 beamline of the storage ring SUPERACO, LURE, Orsay.

2. Experimental

a. Experimental chambers

The experimental setup is composed of two independent chambers connected together.

The preparation part is a "standard" UHV surface chamber fitted with four evaporation sources (Knudsen cells or electron bombardment sources), one of them can be exchanged through a fast-entry lock without breaking the vacuum in the chamber. The evaporation sources are disposed in such a way that all of them can be used simultaneously for co-evaporation on the sample surface. The evaporation rate is determined by a quartz microbalance. During the evaporation process the growth quality can be monitored by RHEED. The sample surface can also be prepared by ion bombardment and annealing (up to 1300 K). The cleanliness and the crystallinity of the sample surface are determined by Auger spectroscopy and LEED, respectively. The preparation chamber is also fitted with a sample fast-entry lock and with a storage place for 6 samples.

The second chamber is dedicated to the conventional and spin-resolved angular photoemission experiments. The chamber is designed as a beamline end-station of synchrotron-radiation storage rings, but, alternatively, we can use UPS and XPS conventional sources mounted in the chamber.

b. Configuration of the photoemission experiment

The schematic view of the electron optics is shown in fig.1a. The energy of emitted photoelectrons is analyzed in a hemispherical (45 mm radius) analyzer (denoted "1" in

fig.1a.) with angular resolution ±1°. At the exit slit of the analyzer two extraction lenses ("2") transfer the electrons to a cylindrical rotator ("3"). Voltages of the rotator can be adjusted to send the electrons either in the transfer optics ("4") and further to the Mott detector or directly in the channeltron fixed behind an opening of the outer cylinder of the rotator.

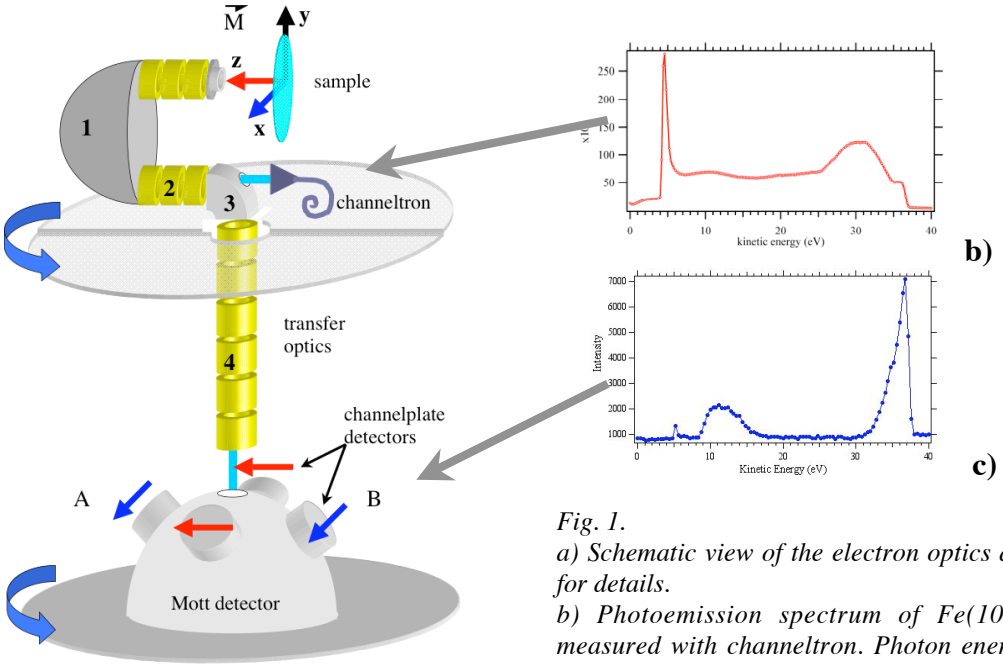

a)

Fig. 1.
a) Schematic view of the electron optics a). See the text for details.
b) Photoemission spectrum of Fe(100) (oxydized) measured with channeltron. Photon energy h□=41 eV, sample current 84 nA, 1 sec/point.
c) Photoemission spectrum of Fe(100) measured with a channelplate. Photon energy h□=42 eV, sample current 84 nA, 6 sec/point.

The channeltron allows performing standard angle-resolved photoemission measurements. It is also very convenient for the preparation of spin-resolved experiments. The counting rate obtained with the channeltron is much higher (typically 10^4 higher) than the counting rate obtained with the Mott detector. We used the channeltron for sample alignment and for a fast check of the sample quality.

The retarding potential Mott ("micro-Mott") detector was designed by Murray Campbell at the University of Edinburgh. It is optimized to operate at 30 kV acceleration voltage; in this case the Sherman function of the system is estimated to be about 0.3 (see fig.9. in: D.M. Campbell et al. J.Phys.E: Sci. Instrum. vol. 18, 1985, 664).

The electrons are impinging on a thin gold layer (about 2000 Å) deposited on a MgO(100) surface.

In the Mott detector two pairs of channelplate assemblies collect the electrons, in order to measure the electron polarization in two perpendicular planes.

The hemispherical analyzer together with all transfer optics and the channeltron (parts "1" to "4") can rotate in the horizontal plane (around the symmetry axis of the transfer optics "4") in order to perform conventional angle-resolved photoemission.
The Mott detector can rotate independently in the horizontal plane as well, which makes it possible to select the component of polarization we want to determine. This possibility of

rotation allows also to get rid of instrumental asymmetries: for a given magnetization of the sample, exchanging channelplates (Mott rotation of 180°, i.e. exchanging channel A and B in fig. 1a) means changing the sign of the measured asymmetry due to electron polarization, but (in principle) not the instrumental asymmetry of the system. This aspect will be also discussed in the following paragraph.

In the given experimental geometry, for normal emission experiments, one can measure *x* and *z* components ("blue" and "red") of the magnetization $\vec{M}$, as schematically shown in fig. 1a. The only possibility measuring the *y* ("black") component is to rotate the sample in azimuth.
In figs. 1b and 1c we show Fe valence-band spectra measured with channeltron and channelplates, respectively.

c. Sample preparation

Our experiments have been performed on a Fe(100) surface. Several high quality iron monocrystals have been prepared by evaporation (about 1000 Å) on MgO(100) substrates. Photoemission experiments show no contamination, as deduced from the form of the spectra close to the binding energy of 6 eV. Crystallinity has been controlled by in-situ LEED patterns and by ex-situ X-ray diffraction measurements. In fig. 2. we show typical LEED patterns characterized by low intensity background and fine diffraction spots.

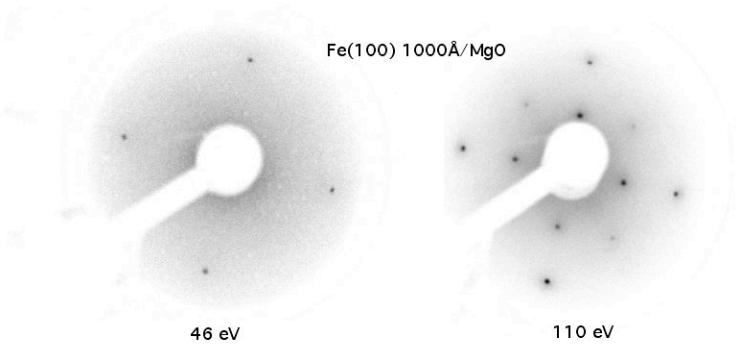

Fig. 2. LEED patterns of the Fe(100) surface measured at two different electron energies.

Magnetic properties of the samples have been checked by ex-situ Kerr-effect experiments. The samples exhibit perfect square-like hysteresis curves with coercitive fields of about 18 oersteds (see fig. 3). The magnetization shows different behavior in MgO(100) and (110) directions.

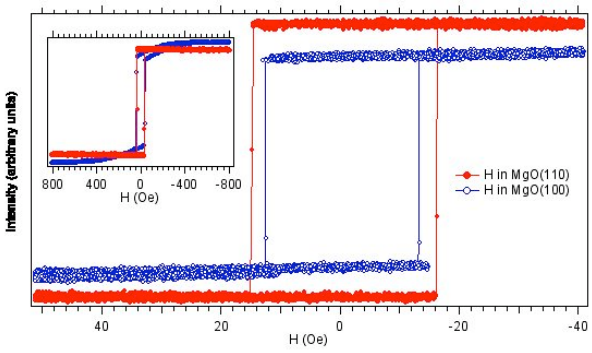

Fig. 3. Kerr-effect measurements on Fe monocrystal. The magnetization easy axis is parallel to the MgO(110) direction which corresponds to the Fe(100) direction.

The easy axis of magnetization appears to be parallel to the MgO(110) direction which is in agreement with the growth of iron on a MgO(100) surface: the Fe lattice is rotated by 45° in comparison with the MgO one.

As shown in the inset of the fig.3. (larger H axis scale), measurements along the MgO(110) direction show a completely flat hysteresis curve in the saturation region, whereas in the MgO(100) direction a higher external magnetic field is needed to reach the saturation.

d. Experiment

The experiments have been performed on the beamline SU6 of the storage ring SUPERACO (†), Orsay. This undulator beamline was very well suited for high flux demanding experiments: it could produce up to 10^{12} photons/sec in the UV energy region. In our measurements we tuned the photon energy to 42 eV (maximum of the first harmonic peak) and the entrance/exit slits were adjusted to 400 and 800 □m, respectively, which gives the resolving power of the beamline of about 1000. In these conditions, we measured a total sample current of about 100 nA (the beamline delivered up to 1 □A in the most favorable conditions: 500/1000 □m entrance/exist slits and 400 mA in the storage ring).

The pass energy of the hemispherical analyzer was of 30 eV and the overall resolution of our measurements was 0.4 eV as estimated from the Fermi step.

In order to maintain high electron flux, in this first set of experiments we removed the entrance slit of the entrance lens system of the hemispherical analyzer which determines the angular resolution. In this configuration the angular resolution is estimated to be about ±7°. All experiments have been done in normal electron emission mode.

We magnetized the samples by applying current pulses to a coil that delivers magnetic fields of about 200 Oe at the sample surface. The samples were always magnetized in (110) direction of the MgO crystal.

All measurements were done at room temperature.

3. Results

Let us just remind that in the spin-resolved photoemission experiment one measures an imbalance between two channels (say, channels materialized by channelplates A and B in fig. 2a) and the polarization P of the electron beam is obtained from the asymmetry A :

$$P = \frac{A}{S} \text{ with } A = \frac{I_A - I_B}{I_A + I_B}, \qquad (1)$$

where S is the Sherman function and I_A and I_B are count rates from channels A and B. Spin-resolved (I_{up}, I_{down}) spectra are then deduced as:

$$I_{up,down} = I_0(1 \pm P) = I_0(1 \pm \frac{A}{S}). \qquad (2)$$

I_0 is the spin-integrated spectrum $I_0 = (I_A + I_B)/2$.

In our experimental conditions, as mentioned in §2.d, the typical channelplate count rate was of about 1000 counts/second. Comparing the count rates from the channeltron and from the channelplates for the same experimental conditions, we can deduce that the transfer optics ("4" in the fig.1a) transmits the electron beam without losses.

In order to check properly the functionalities of the system we preformed experiments in different situations. We first measured a non-magnetized sample, just after Fe evaporation on a MgO monocrystal. Then we determined the asymmetry A in the four possible situations:

- for a given position of channelplates we reversed the sample magnetization $\vec{M}$.
- for a given magnetization $\vec{M}$ of the sample we reversed the positions of the channelplates (i.e. rotating the Mott detector by 180°, see fig. 1.a)

In fig. 4a we show a spectrum measured (accumulation 20 sec/point) by one of the channelplates, in fig. 4b the asymmetry for a non-magnetized sample and in fig. 4c the asymmetries obtained after magnetizing the sample in two opposed directions. One can see that when changing the magnetization the asymmetries in fig. 4c are reversed, but the mirror line is not the zero line. This is due to the instrumental asymmetry of the system.
We verified that reversing the channelplate positions (i.e. rotating the Mott detector by 180°) for the same magnetization gives the same form and amplitude of the reversed asymmetry.

The asymmetries were calculated from the spectra after subtraction of a constant background.

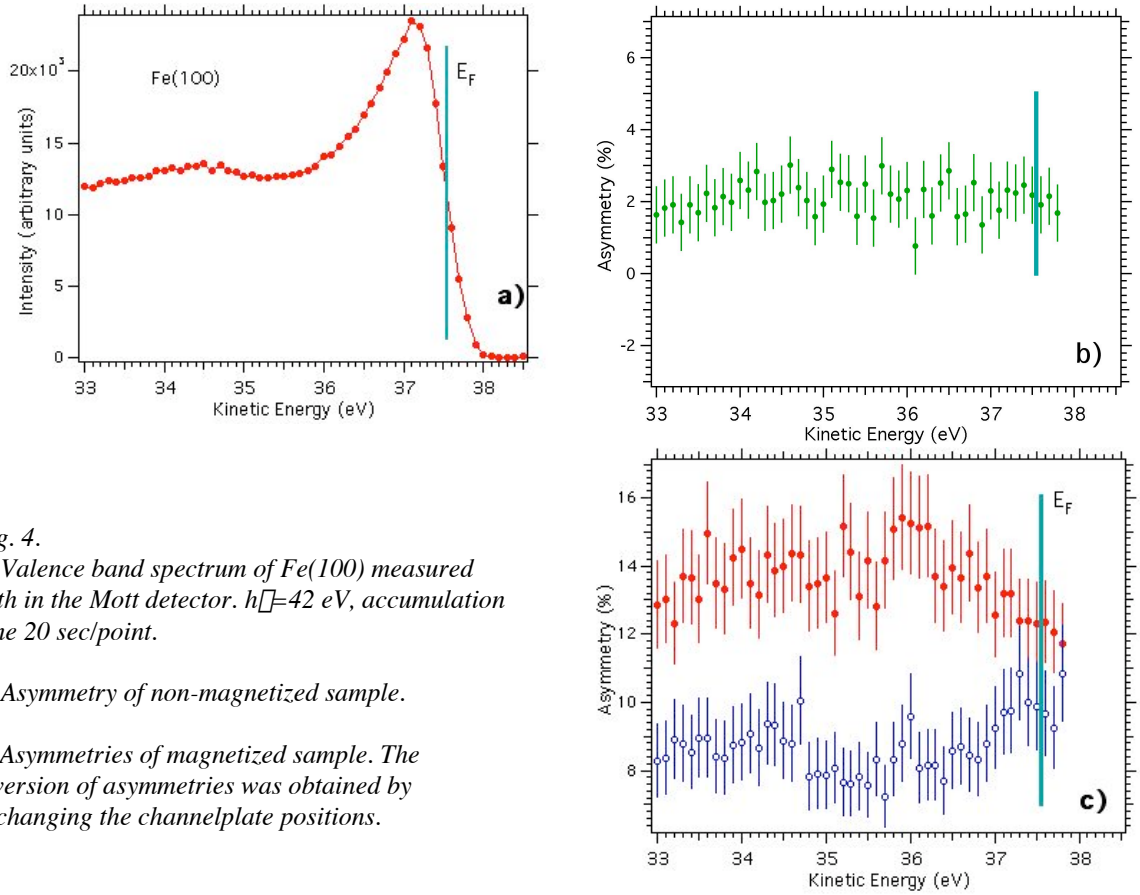

Fig. 4.
a) Valence band spectrum of Fe(100) measured with in the Mott detector. h□=42 eV, accumulation time 20 sec/point.

b) Asymmetry of non-magnetized sample.

c) Asymmetries of magnetized sample. The inversion of asymmetries was obtained by exchanging the channelplate positions.

After having completed the measurements for all four possible configurations (opposite magnetizations and opposite channelplate positions) we can remove the instrumental asymmetry by subtracting the measurements with opposite channelplate position giving opposite asymmetries, as shown in fig. 5. Now, the zero line is mirror line for the asymmetries in within the error bars.

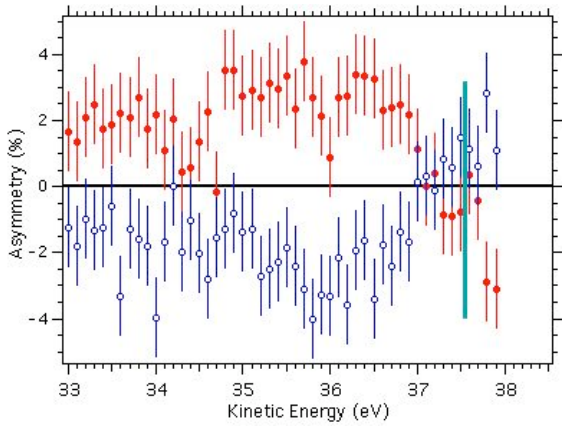

Fig. 5.
Asymmetries measured with opposed magnetizations. For both cases the instrumental asymmetry was removed by subtraction of the asymmetries measured with inversed channelplate positions . Accumulation time 20 sec/point.

We can compare now our results with those already reported in literature, as shown in fig.6. In fig. 6a we display the asymmetry obtained with our detector for 80 sec/point count rate, in fig. 6b we present the polarization measured by Kisker and Carbone. Qualitatively both curves show the same behavior.

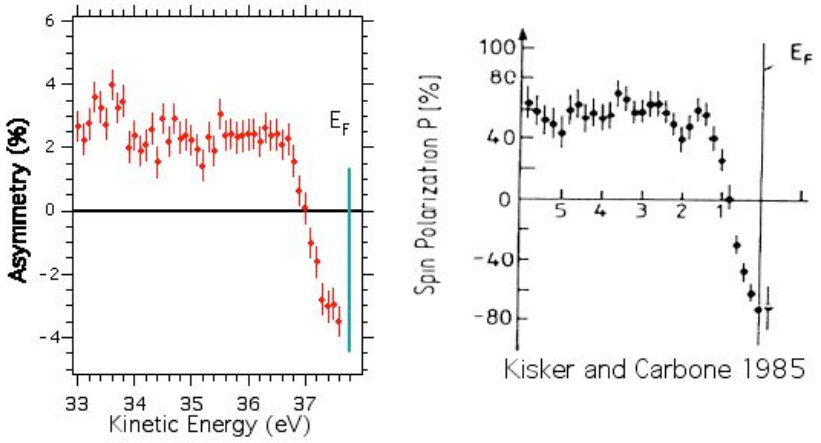

Fig. 6.
Comparison of our measurements (accumulation time 80 sec/point) with the literature.

The y-scales are different by a factor that corresponds to the Sherman function of our Mott detector. Comparing both graphs gives us an estimate of our Sherman function of 0.05, which is much smaller than the one expected for our type of Mott detector. The reason for this loss of value for our Sherman function is mainly due to two points:

1) For all reported results here we were obliged to reduce the high voltage (leak currents at high voltages) in the Mott detector to 18 kV (nominal value is 30 kV), which reduces the Sherman function.

2) Magnetization in our samples has only in plane components and as we have magnetized in the horizontal direction, the measurable component is parallel to the x-axis ("blue" component in fig. 1a). We rotated the Mott detector in order to measure only this component (with channelplates A and B in fig. 1a). In fact, we obtained an asymmetry also in the perpendicular plane, i.e. as if a component perpendicular to the surface, i.e. in the *z* direction ("red" in fig. 1a) was non-zero. During this set of measurements there was no shielding for external magnetic fields in our experimental chamber, so the appearance of the perpendicular component of magnetization can be explained by a precession of the electron spins due to the presence of a magnetic field. In between we have built a set of coils for compensation of this external field and new experiments are in progress.

Finally we present in fig. 7 spin-resolved spectra calculated using equation (2). They nicely reproduce the results obtained in similar conditions (Kisker et al. PRB 31 (1985), 329).

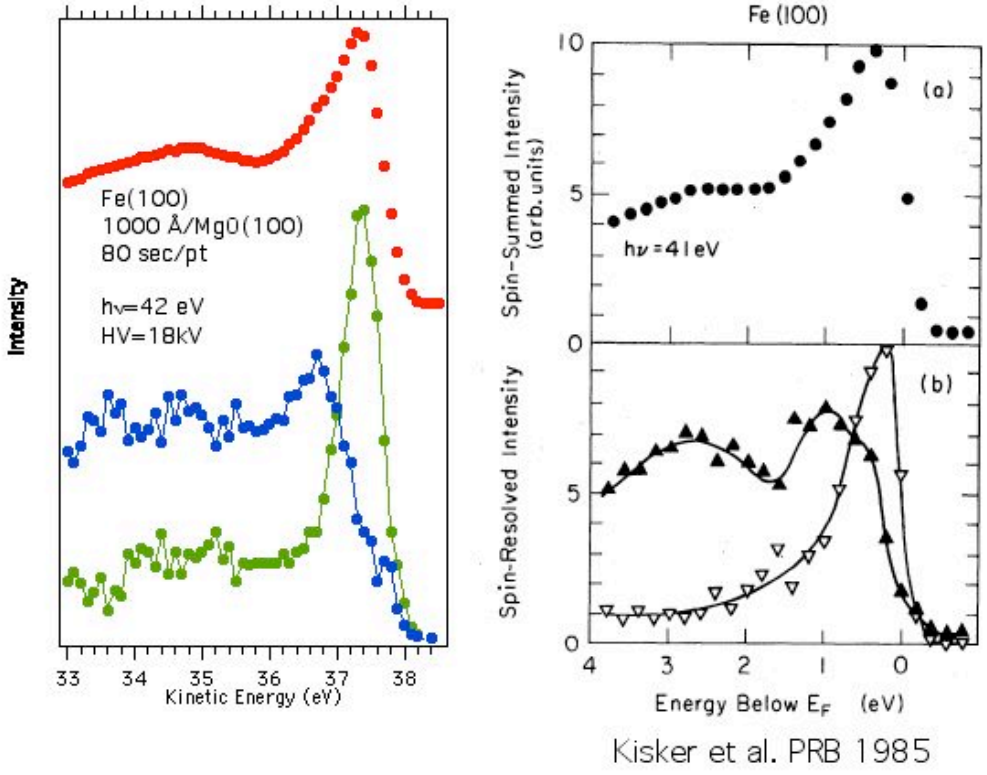

Fig.7. Calculated spin-resolved spectra and comparison with literature.